Three-point combined compact difference schemes for time-fractional advection-diffusion equations with smooth solutions☆

Guang-Hua Gao[a], Hai-Wei Sun[b,*]

[a] *College of Science, Nanjing University of Posts and Telecommunications, Nanjing 210023, P. R. China*
[b] *Department of Mathematics, University of Macau, Macao*

Abstract

In this paper, we study the numerical solution for the time-fractional advection-diffusion equation (TFADE). A high-order accurate three-point combined compact difference scheme with the *L1 formula* is proposed to solve a class of TFADEs. The method is globally $(2-\gamma)$th-order accurate in time and at least fifth-order accurate in space for the constant coefficient TFADEs subject to periodic boundary conditions, where γ is the order of time-fractional derivative in the governing equation. The unconditional stability and the high-order convergence are proved using the Fourier analysis method. The proposed method can be extended to treat the variable coefficient TFADEs subject to other local boundary conditions. Several numerical examples are computed to validate the numerical accuracy, effectiveness and robustness of the present method for TFADEs with smooth solutions and different boundary conditions. Moreover, the proposed algorithm preserves the higher order accuracy for advection-dominated problems with the smooth solutions.

Keywords: Time-fractional advection-diffusion equations; *L1 formula*; Combined compact difference scheme; Stability; Convergence

1. Introduction

The fractional operator is non-local and it considers the historic distributed effects. Numerous applications and physical manifestations promote the development of fractional calculus in the past few decades. Various fractional partial differential equations have been established to depict phenomenons in fields of engineering, science and economics, such as carrier transport in amorphous semiconductors, system identification and control, anomalous diffusion in electrochemistry, fractance circuits, electrode electrolyte interface, viscoelasticity, fractional neural modeling in bio-sciences, chaos theory, finance and so on [1, 2, 3, 4, 5, 6].

☆The research was supported by the research grant 11271068, 11326225, 11401319 from National Natural Science Foundation of China, BK20130860 from Natural Science Youth Foundation of Jiangsu Province, NY213051 from the Scientific Research Foundation of Nanjing University of Posts and Telecommunications, 105/2012/A3 from FDCT of Macao, and MYRG102(Y2-L3)-FST13-SHW from University of Macau.

*Corresponding author
Email addresses: gaoguanghua1107@163.com (Guang-Hua Gao), HSun@umac.mo (Hai-Wei Sun)

For most time-fractional advection-diffusion equations (TFADEs), it is not an easy task to seek for their analytical solutions. Although they are available for some simple cases, the solutions often refer to some special functions, which are quite sophisticated in calculation. Therefore, it is essential to survey the effective numerical solutions of TFADEs. Recently, a tremendous amount of works were devoted to the finite difference methods for solving the fractional differential equations. Yuste and Acedo [7] established an explicit difference scheme for solving the fractional sub-diffusion equations, with the Grünwald-Letnikov approximation for the Riemann-Liouville time-fractional derivative and a forward Euler approximation for the first-order time derivative. The von Neumann-type analysis is applied to determine stability conditions of the obtained difference scheme. For the same fractional sub-diffusion equations with Neumann boundary conditions (NBCs), Langlands and Henry [8] presented an implicit difference scheme with the *L1* approximation for the Riemann-Liouville time-fractional derivative and a backward Euler approximation for the first-order time derivative. Although the accuracy to approximate the time-fractional derivative was improved from order one to order $2-\gamma$ for the Riemann-Liouville fractional derivative of order γ $(0<\gamma<1)$, the whole numerical accuracy of difference scheme still kept order one due to the first-order Euler approximation for the first-order time derivative. Liu [9] also investigated an implicit difference approach by combining the *L1 formula* for the Caputo time-fractional derivative of order γ and the second-order central difference quotient for the second-order space derivative. Nevertheless, only the first-order convergence in time was proved by the discrete maximum principle. Sun and Wu [10] discussed the unconditionally stable difference schemes for fractional diffusion-wave equations using the *L1 formula* to approximate the Caputo time-fractional derivatives. The rigorous proof for numerical accuracy of the *L1 formula* was given in [10]. The proof of this formula was also drawn by another way during the discussion of spectral methods for the fractional sub-diffusion [11] and the fractional cable equations [12]. For the fractional sub-diffusion problem, Chen et al. [13] developed an implicit difference scheme using the first-order Grünwald-Letnikov approximation for the Riemann-Liouville time-fractional derivative and analyzed the scheme by the Fourier method. An implicit moving least squares meshless method was used to solve the time-dependent fractional advection-diffusion equations in [14]. About more relevant work on the subject, readers can refer to the literatures [15, 16, 17] and references therein.

As we have mentioned above, the fractional operator is non-local and with memory of history. For the time-fractional differential equations, when computing the values of unknowns on the current time level, all function values of unknowns on previous time levels need to be stored. Therefore, it is important and meaningful to develop some higher-order accurate numerical methods for solving the time fractional differential equations. In 2009, Cui [18] constructed a compact difference scheme with the first-order accuracy in time and fourth-order accuracy in space for solving a fractional sub-diffusion equation. Later, Du, Cao and Sun [19], Gao and Sun [20], Hu and Zhang [21, 22], Mohebbi and Abbaszadeh [23], and Ren, Sun and Zhao [24] studied the spatial fourth-order compact schemes for solving several types of time-fractional partial differential equations. All above compact difference schemes are only constructed for Dirichlet boundary value problems (except [24] which considered

the NBCs) and achieve the fourth-order numerical accuracy in space. Recently, some new works on the higher-order numerical approximation for the time-fractional derivatives can also be found. Cao and Xu [25] obtained a higher-order scheme for the numerical solution of the fractional ordinary differential equations starting from the equivalent integral form of the original differential equations. Gao and Sun [26] proposed a new *L1-2 formula* to approximate the Caputo time-fractional derivatives and investigated the applications of this formula into solving fractional differential equations. Zeng et al. [27] presented the fractional linear multistep method for the discretization of the time-fractional derivatives. Li and Ding [28] used the Grünwald formula with the coefficients generated from the quadratic polynomial to improve the numerical accuracy for approximating the time-fractional derivatives. Wang and Vong [29] developed the high-order difference schemes for the modified anomalous fractional sub-diffusion equation and the fractional diffusion-wave equation using the weighted and shifted Grünwald formula.

In 1998, Chu and Fan [30] proposed a combined compact difference (CCD) method for solving 1D and 2D steady convection diffusion equations. The CCD method in [30] is an implicit three-point scheme, with the sixth-order accuracy of local truncated approximation, which can be efficiently solved by the so-called triple-tridiagonal solver [30]. In related numerical methods for solving the partial differential equations by the CCD scheme, the first- and second-order derivatives together with the function values of unknowns at grid points are computed simultaneously. More developments on the CCD method can be found in [31, 32, 33, 34, 35]. Nevertheless, to our knowledge, the three-point CCD scheme has never been employed to solve the time-fractional partial differential equations before. Moreover, the global convergence analysis of the CCD scheme was not studied in the literature.

In this paper, we propose the three-point CCD scheme along with the *L1 formula* for solving the 1D TFADEs. The choice of the *L1 formula* for approximating the time-fractional derivatives is due to the good properties of coefficients in this formula which facilitate the theoretical analysis on the corresponding schemes. At first, we investigate the constant coefficient TFADE subject to the periodic boundary condition (PBC) using the Fourier analysis method. For this case, the unconditional stability, the global at least fifth-order accuracy in space and the global $(2-\gamma)$th-order accuracy in time of the proposed method are theoretically proved. Then we extend the proposed method to the variable coefficient cases with other local boundary conditions. As we know, it is quite complicated to apply the fourth-order Padé-type compact technique for fractional diffusion or cable equations [18, 19, 20, 21, 22] to construct the compact difference scheme for variable coefficient and advection-diffusion equations, especially for the non self-adjoint cases. Here, the CCD scheme will be evolved from attempts to alleviate these disadvantages and to provide a perspective for the establishment of some higher-order accurate difference schemes for solving some variable coefficient and advection-diffusion equations. We also show the $(2-\gamma)$th order local accuracy in time and the higher-order local accuracy in space of the proposed methods. We remark that for derivative boundary value problems, such as the problems with NBCs or mixed boundary conditions, we do not need to especially discretize the derivative boundary conditions anymore, which is usually the one of difficult points by the general compact finite difference

methods for these problems in which the space derivatives are directly discretized using the difference quotient. Numerical experiments show that the proposed CCD scheme for 1D TFADEs can maintain the good computational efficiency even for advection-dominated problems with the smooth solutions.

The remainder is arranged as follows. In section 2, the CCD scheme for the constant coefficient TFADEs subject to PBC is proposed. The stability and global convergence of the resultant CCD scheme are also analyzed by the Fourier method. The global convergence analysis on the CCD scheme, even for the problem of integer order, has not been seen before by the authors. In section 3, the CCD scheme is presented for more general variable coefficient TFADEs subject to three different kinds of boundary conditions, respectively. Several numerical examples are given in section 4 to verify the effectiveness and numerical accuracy of the newly developed CCD schemes. A brief conclusion and future work will appear finally.

2. Constant coefficient TFADEs subject to PBC

In this section, we study the following TFADEs

$$
\begin{aligned}
&{}_0^C\mathcal{D}_t^\gamma \theta(x,t) = \kappa_1 \theta_{xx}(x,t) - \kappa_2 \theta_x(x,t) + f(x,t), \quad x \in \mathbb{R} = [-\infty, \infty],\ t \in (0,T], && (2.1)\\
&\theta(x,0) = \theta_0(x), \quad x \in \mathbb{R}, && (2.2)
\end{aligned}
$$

subject to the L-PBC

$$
\theta(x,t) = \theta(x+L,t), \quad x \in \mathbb{R},\ t \in [0,T], \tag{2.3}
$$

where κ_1, κ_2, L, γ are constants, $\kappa_1 > 0$, $L > 0$, $0 < \gamma < 1$ and ${}_0^C\mathcal{D}_t^\gamma$ is the Caputo fractional derivative of order γ defined by

$$
{}_0^C\mathcal{D}_t^\gamma u(t) = \frac{1}{\Gamma(1-\gamma)} \int_0^t \frac{u'(s)}{(t-s)^\gamma}\, \mathrm{d}s.
$$

Some further applications of the CCD scheme into more generalized TFADEs, readers can proceed with concerning on our work in section 3.

To solve the periodic initial-boundary value problem (2.1)–(2.3), one can restrict it on a bounded domain $\Omega = [0, L] \times [0, T]$. On the domain Ω, denote $x_j = jh$ $(0 \leqslant j \leqslant M+1)$ with $h = L/M$, $t_k = k\tau$ $(0 \leqslant k \leqslant N)$ with $\tau = T/N$, where M, N are two positive integers. Define the mesh function spaces $\Omega_h = \{x_i \mid 0 \leqslant i \leqslant M\}$, $\Omega_\tau = \{t_k \mid 0 \leqslant k \leqslant N\}$. Then the computational domain Ω is covered by $\Omega_h \times \Omega_\tau$.

For any mesh function $u = \{u^k \mid 0 \leqslant k \leqslant N\}$ defined on the mesh space Ω_τ, introducing a notation [20]

$$
D_t^\gamma u^k = \frac{\tau^{-\gamma}}{\Gamma(2-\gamma)} \Big[\lambda_0^{(\gamma)} u^k - \sum_{l=1}^{k-1} (\lambda_{k-l-1}^{(\gamma)} - \lambda_{k-l}^{(\gamma)}) u^l - \lambda_{k-1}^{(\gamma)} u^0 \Big], \tag{2.4}
$$

where

$$\lambda_j^{(\gamma)} = (j+1)^{1-\gamma} - j^{1-\gamma}, \quad j \geqslant 0. \tag{2.5}$$

Here, D_t^γ is a discretized operator for the Caputo time-fractional derivative operator ${}_0^C\mathcal{D}_t^\gamma$ and it is usually called the *L1* approximation operator. The *L1* approximation operator is obtained by the piecewise linear approximation of the function $u(t)$ and its numerical accuracy is $O(\tau^{2-\gamma})$ if $u(t) \in C^2[0, t_k]$. The following lemma states the fact.

Lemma 1. *[10, 20, 37] Suppose $u(t) \in C^2[0, t_k]$. Let*

$$\overline{R}\big(u(t_k)\big) := {}_0^C\mathcal{D}_t^\gamma u(t)|_{t=t_k} - D_t^\gamma u(t_k),$$

then

$$|\overline{R}\big(u(t_k)\big)| \leqslant \frac{1}{\Gamma(2-\gamma)}\Big[\frac{1-\gamma}{12} + \frac{2^{2-\gamma}}{2-\gamma} - (1+2^{-\gamma})\Big] \max_{0\leqslant t\leqslant t_k} |u''(t)|\tau^{2-\gamma},$$

where $0 < \gamma < 1$ and D_t^γ is defined by (2.4).

2.1. The three-point CCD scheme

The CCD method [30] is established using a local Hermitian polynomial approximation for the function $u(x)$ on each small interval $[x_{j-1}, x_{j+1}]$. In fact, the derivation of these relationships can be obtained easily by Taylor's theorem (see Appendix part). More precisely, if $u(x) \in C^8[x_{j-1}, x_{j+1}]$, with notations $u_j = u(x_j), u_j' = u'(x_j), u_j'' = u''(x_j)$, these equalities are expressed by

$$\frac{7}{16}(u_{j+1}' + u_{j-1}') + u_j' - \frac{h}{16}(u_{j+1}'' - u_{j-1}'') = \frac{15}{16h}(u_{j+1} - u_{j-1}) + \mathcal{O}(h^6), \tag{2.6}$$

$$\frac{9}{8h}(u_{j+1}' - u_{j-1}') - \frac{1}{8}(u_{j+1}'' + u_{j-1}'') + u_j'' = \frac{3}{h^2}(u_{j+1} - 2u_j + u_{j-1}) + \mathcal{O}(h^6). \tag{2.7}$$

These relationships involve only three points x_{j-1}, x_j, x_{j+1} in the stencil and the compact structure is preserved. The dominated truncation terms of (2.6) and (2.7) are sixth-order. In other words, these expressions can be taken into account for solving the numerical solutions of differential equations based on their compact structure and high accuracy after neglecting small terms.

Suppose $\theta(x,t) \in C^{8,2}(\Omega)$. Define the grid functions

$$\Theta_j^k = \theta(x_j, t_k), \quad (\Theta_x)_j^k = \theta_x(x_j, t_k),$$

$$(\Theta_{xx})_j^k = \theta_{xx}(x_j, t_k), \quad f_j^k = f(x_j, t_k),\ 0 \leqslant j \leqslant M+1,\ 0 \leqslant k \leqslant N.$$

The combination of the *L1* approximation (2.4) for the time-fractional derivative and the three-point CCD approximation (2.6)–(2.7) for the spatial first- and second-order derivatives

produces the following expressions:

$$D_t^\gamma \Theta_j^k = \kappa_1 (\Theta_{xx})_j^k - \kappa_2 (\Theta_x)_j^k + f_j^k + R_j^k, \quad 1 \leqslant j \leqslant M,\ 1 \leqslant k \leqslant N, \tag{2.8}$$

$$\frac{7}{16}[(\Theta_x)_{j+1}^k + (\Theta_x)_{j-1}^k] + (\Theta_x)_j^k - \frac{h}{16}[(\Theta_{xx})_{j+1}^k - (\Theta_{xx})_{j-1}^k] = \frac{15}{16h}(\Theta_{j+1}^k - \Theta_{j-1}^k) + S_j^k,$$
$$1 \leqslant j \leqslant M,\ 1 \leqslant k \leqslant N, \tag{2.9}$$

$$\frac{9}{8h}[(\Theta_x)_{j+1}^k - (\Theta_x)_{j-1}^k] - \frac{1}{8}[(\Theta_{xx})_{j+1}^k + (\Theta_{xx})_{j-1}^k] + (\Theta_{xx})_j^k = \frac{3}{h^2}(\Theta_{j+1}^k - 2\Theta_j^k + \Theta_{j-1}^k) + T_j^k,$$
$$1 \leqslant j \leqslant M,\ 1 \leqslant k \leqslant N, \tag{2.10}$$

$$\Theta_j^0 = \theta_0(x_j), \quad 1 \leqslant j \leqslant M, \tag{2.11}$$

where by Lemma 1 and (2.6)–(2.7), there exists a positive constant c such that

$$|R_j^k| \leqslant c\,\tau^{2-\gamma}, \quad |S_j^k| \leqslant c\,h^6, \quad |T_j^k| \leqslant c\,h^6, \quad 1 \leqslant j \leqslant M,\ 1 \leqslant k \leqslant N. \tag{2.12}$$

Omitting the small terms R_j^k, S_j^k and T_j^k in (2.8)–(2.11), a high-order three-point CCD scheme for solving (2.1)–(2.3) on Ω is obtained as follows:

$$D_t^\gamma \theta_j^k = \kappa_1 (\theta_{xx})_j^k - \kappa_2 (\theta_x)_j^k + f_j^k, \quad 1 \leqslant j \leqslant M,\ 1 \leqslant k \leqslant N, \tag{2.13}$$

$$\frac{7}{16}[(\theta_x)_{j+1}^k + (\theta_x)_{j-1}^k] + (\theta_x)_j^k - \frac{h}{16}[(\theta_{xx})_{j+1}^k - (\theta_{xx})_{j-1}^k] = \frac{15}{16h}(\theta_{j+1}^k - \theta_{j-1}^k),$$
$$1 \leqslant j \leqslant M,\ 1 \leqslant k \leqslant N, \tag{2.14}$$

$$\frac{9}{8h}[(\theta_x)_{j+1}^k - (\theta_x)_{j-1}^k] - \frac{1}{8}[(\theta_{xx})_{j+1}^k + (\theta_{xx})_{j-1}^k] + (\theta_{xx})_j^k = \frac{3}{h^2}(\theta_{j+1}^k - 2\theta_j^k + \theta_{j-1}^k),$$
$$1 \leqslant j \leqslant M,\ 1 \leqslant k \leqslant N, \tag{2.15}$$

$$\theta_j^0 = \theta_0(x_j), \quad 1 \leqslant j \leqslant M. \tag{2.16}$$

At each time level t_k ($1 \leqslant k \leqslant N$), the difference scheme (2.13)–(2.16) is a linear algebraic system with respect to the unknowns $[\theta_{\mathbf{x}}^{\mathbf{k}}, \theta_{\mathbf{xx}}^{\mathbf{k}}, \theta^{\mathbf{k}}]^T$ with $\theta_{\mathbf{x}}^{\mathbf{k}} = [(\theta_x)_1^k, (\theta_x)_2^k, \ldots, (\theta_x)_M^k]$, $\theta_{\mathbf{xx}}^{\mathbf{k}} = [(\theta_{xx})_1^k, (\theta_{xx})_2^k, \ldots, (\theta_{xx})_M^k]$ and $\theta^{\mathbf{k}} = [\theta_1^k, \theta_2^k, \ldots, \theta_M^k]$. The coefficient matrix of the system can be arranged as the triple-tridiagonal structure except several individual elements for the boundary nodes and the system can be solved by two steps: triple-forward elimination and triple-backward substitution. More details can be found in [30].

2.2. Analysis of the difference scheme (2.13)–(2.16)

In this section, the stability and the global convergence of difference scheme (2.13)–(2.16) are investigated. First, a lemma about the properties of coefficients $\lambda_j^{(\gamma)} (j \geqslant 0)$ defined in (2.5) is set out.

Lemma 2. *[20, 37, 38] Suppose* $0 < \gamma < 1$ *and* $\lambda_j^{(\gamma)}$ *is defined by* (2.5), $j = 0, 1, \ldots$. *Then*

(1) $1 = \lambda_0^{(\gamma)} > \lambda_1^{(\gamma)} > \lambda_2^{(\gamma)} > \cdots > \lambda_j^{(\gamma)} \to 0$, *as* $j \to +\infty$;

(2) $\lambda_{k-1}^{(\gamma)} > (1-\gamma)k^{-\gamma}$.

Second, for any mesh function $u = [u_0, u_1, \ldots, u_M]^T$ on Ω_h, define

$$\|u\| = \sqrt{h \sum_{j=1}^{M} u_j^2}.$$

Next, a prior estimate theorem is given.

Theorem 1. *(Prior estimate) Suppose $\{u_j^k\}, \{v_j^k\}$ and $\{w_j^k\}$ $(1 \leqslant j \leqslant M,\ 0 \leqslant k \leqslant N)$ are the solutions of*

$$D_t^\gamma u_j^k = \kappa_1 w_j^k - \kappa_2 v_j^k + f_j^k, \quad 1 \leqslant j \leqslant M,\ 1 \leqslant k \leqslant N, \tag{2.17}$$

$$\frac{7}{16}(v_{j+1}^k + v_{j-1}^k) + v_j^k - \frac{h}{16}(w_{j+1}^k - w_{j-1}^k) = \frac{15}{16h}(u_{j+1}^k - u_{j-1}^k) + g_j^k,$$
$$1 \leqslant j \leqslant M,\ 1 \leqslant k \leqslant N, \tag{2.18}$$

$$\frac{9}{8h}(v_{j+1}^k - v_{j-1}^k) - \frac{1}{8}(w_{j+1}^k + w_{j-1}^k) + w_j^k = \frac{3}{h^2}(u_{j+1}^k - 2u_j^k + u_{j-1}^k) + \widetilde{g}_j^k,$$
$$1 \leqslant j \leqslant M,\ 1 \leqslant k \leqslant N, \tag{2.19}$$

$$u_j^0 = u_0(x_j), \quad 1 \leqslant j \leqslant M. \tag{2.20}$$

Then it holds

$$\|u^k\|^2 \leqslant 2\|u^0\|^2 + 6T^{2\gamma}\Gamma^2(1-\gamma) \max_{1 \leqslant l \leqslant N} \Big[\|f^l\|^2 + (4\kappa_1^2 + 16\kappa_2^2 h^2/25)\|\widetilde{g}^l\|^2 \tag{2.20}$$
$$+ (64\kappa_2^2 + 36\kappa_1^2/h^2)\|g^l\|^2\Big], \quad 1 \leqslant k \leqslant N. \tag{2.21}$$

Proof. At the beginning, the vectors of solutions

$$u^k = [u_1^k, u_2^k, \ldots, u_M^k]^T, v^k = [v_1^k, v_2^k, \ldots, v_M^k]^T, w^k = [w_1^k, w_2^k, \ldots, w_M^k]^T,\ 0 \leqslant k \leqslant N,$$

can be expanded into piecewise constant functions in the following way, respectively,

$$u^k(x) = \begin{cases} u_j^k, & x_j - \dfrac{h}{2} \leqslant x < x_j + \dfrac{h}{2},\ 1 \leqslant j \leqslant M-1, \\ u_M^k, & x \in [x_M - \dfrac{h}{2}, x_M] \cup [x_0, x_0 + \dfrac{h}{2}); \end{cases}$$

$$v^k(x) = \begin{cases} v_j^k, & x_j - \dfrac{h}{2} \leqslant x < x_j + \dfrac{h}{2},\ 1 \leqslant j \leqslant M-1, \\ v_M^k, & x \in [x_M - \dfrac{h}{2}, x_M] \cup [x_0, x_0 + \dfrac{h}{2}); \end{cases}$$

$$w^k(x) = \begin{cases} w_j^k, & x_j - \dfrac{h}{2} \leqslant x < x_j + \dfrac{h}{2},\ 1 \leqslant j \leqslant M-1, \\ w_M^k, & x \in [x_M - \dfrac{h}{2}, x_M] \cup [x_0, x_0 + \dfrac{h}{2}); \end{cases}$$

$f^k(x), g^k(x), \widetilde{g}^k(x)$ are defined similarly.

On $[0, L]$, we expand $u^k(x), v^k(x), w^k(x),\ f^k(x), g^k(x), \widetilde{g}^k(x)$ into Fourier series, respectively, as

$$u^k(x) = \frac{1}{\sqrt{L}} \sum_{m=-\infty}^{\infty} a_k(m) e^{\mathbf{i}2\pi mx/L}, \quad v^k(x) = \frac{1}{\sqrt{L}} \sum_{m=-\infty}^{\infty} b_k(m) e^{\mathbf{i}2\pi mx/L},$$

$$w^k(x) = \frac{1}{\sqrt{L}} \sum_{m=-\infty}^{\infty} c_k(m) e^{\mathbf{i}2\pi mx/L}, \quad f^k(x) = \frac{1}{\sqrt{L}} \sum_{m=-\infty}^{\infty} p_k(m) e^{\mathbf{i}2\pi mx/L},$$

$$g^k(x) = \frac{1}{\sqrt{L}} \sum_{m=-\infty}^{\infty} q_k(m) e^{\mathbf{i}2\pi mx/L}, \quad \widetilde{g}^k(x) = \frac{1}{\sqrt{L}} \sum_{m=-\infty}^{\infty} r_k(m) e^{\mathbf{i}2\pi mx/L}, \quad 0 \leqslant k \leqslant N,$$

where $\mathbf{i}$ is the imaginary unit, and

$$a_k(m) = \frac{1}{\sqrt{L}} \int_0^L u^k(x) e^{-\mathbf{i}2\pi mx/L}\,\mathrm{d}x, \quad b_k(m) = \frac{1}{\sqrt{L}} \int_0^L v^k(x) e^{-\mathbf{i}2\pi mx/L}\,\mathrm{d}x,$$

$$c_k(m) = \frac{1}{\sqrt{L}} \int_0^L w^k(x) e^{-\mathbf{i}2\pi mx/L}\,\mathrm{d}x, \quad p_k(m) = \frac{1}{\sqrt{L}} \int_0^L f^k(x) e^{-\mathbf{i}2\pi mx/L}\,\mathrm{d}x,$$

$$q_k(m) = \frac{1}{\sqrt{L}} \int_0^L g^k(x) e^{-\mathbf{i}2\pi mx/L}\,\mathrm{d}x, \quad r_k(m) = \frac{1}{\sqrt{L}} \int_0^L \widetilde{g}^k(x) e^{-\mathbf{i}2\pi mx/L}\,\mathrm{d}x.$$

Then, by the definition of continuous L^2 norm and the Parseval equality, it follows

$$\|u^k(x)\|_{L^2}^2 = \int_0^L |u^k(x)|^2\,\mathrm{d}x = \sum_{m=-\infty}^{\infty} |a_k(m)|^2.$$

Noticing the definition of discrete L^2 norm for u^k, we get

$$\begin{aligned}\|u^k\|^2 = h\sum_{j=1}^{M}(u_j^k)^2 &= \int_{x_0}^{x_0+\frac{h}{2}} [u^k(x)]^2\,\mathrm{d}x + \sum_{j=1}^{M-1} \int_{x_j-\frac{h}{2}}^{x_j+\frac{h}{2}} [u^k(x)]^2\,\mathrm{d}x + \int_{x_M-\frac{h}{2}}^{x_M} [u^k(x)]^2\,\mathrm{d}x \\ &= \|u^k(x)\|_{L^2}^2.\end{aligned}$$

It yields from the above process that

$$\|u^k\|^2 = \sum_{m=-\infty}^{\infty} |a_k(m)|^2. \tag{2.22}$$

Similarly, for $0 \leqslant k \leqslant N$, it holds that

$$\|v^k\|^2 = \sum_{m=-\infty}^{\infty} |b_k(m)|^2, \quad \|w^k\|^2 = \sum_{m=-\infty}^{\infty} |c_k(m)|^2,$$

$$\|f^k\|^2 = \sum_{m=-\infty}^{\infty} |p_k(m)|^2, \quad \|g^k\|^2 = \sum_{m=-\infty}^{\infty} |q_k(m)|^2, \quad \|\widetilde{g}^k\|^2 = \sum_{m=-\infty}^{\infty} |r_k(m)|^2.$$

Based on the above analysis, we can suppose

$$u_j^k = \frac{1}{\sqrt{L}} a_k e^{\mathbf{i}\rho j h}, \quad v_j^k = \frac{1}{\sqrt{L}} b_k e^{\mathbf{i}\rho j h}, \quad w_j^k = \frac{1}{\sqrt{L}} c_k e^{\mathbf{i}\rho j h},$$

$$f_j^k = \frac{1}{\sqrt{L}} p_k e^{\mathbf{i}\rho j h}, \quad g_j^k = \frac{1}{\sqrt{L}} q_k e^{\mathbf{i}\rho j h}, \quad \widetilde{g}_j^k = \frac{1}{\sqrt{L}} r_k e^{\mathbf{i}\rho j h},$$

where $\rho = 2m\pi/L$.

From (2.18) and (2.19), for $1 \leqslant k \leqslant N$, we arrive at

$$\Big[1 + \frac{7}{8}\cos(\rho h)\Big] b_k - \mathbf{i}\frac{h}{8}\sin(\rho h) c_k = \mathbf{i}\frac{15}{8h}\sin(\rho h) a_k + q_k, \tag{2.23}$$

$$\mathbf{i}\frac{9}{4h}\sin(\rho h) b_k + \Big[1 - \frac{1}{4}\cos(\rho h)\Big] c_k = \frac{6}{h^2}[\cos(\rho h) - 1] a_k + r_k. \tag{2.24}$$

A straightforward calculation produces that

$$b_k = \mathbf{i}\frac{1}{h}\phi_1\Big(\cos(\rho h), \sin(\rho h)\Big) a_k + \mathbf{i}\varphi_1\Big(\cos(\rho h), \sin(\rho h)\Big) r_k + \psi_1\Big(\cos(\rho h)\Big) q_k, \tag{2.25}$$

$$c_k = \frac{1}{h^2}\phi_2\Big(\cos(\rho h)\Big) a_k + \varphi_2\Big(\cos(\rho h)\Big) r_k - \mathbf{i}\psi_2\Big(\cos(\rho h), \sin(\rho h)\Big) q_k, \tag{2.26}$$

where

$$\phi_1(x,y) = \frac{9y(4+x)}{2x^2+20x+23}, \ \varphi_1(x,y) = \frac{4hy}{2x^2+20x+23}, \ \psi_1(x) = \frac{8(4-x)}{2x^2+20x+23},$$

$$\phi_2(x) = \frac{3(11x^2+8x-19)}{2x^2+20x+23}, \ \varphi_2(x) = \frac{4(7x+8)}{2x^2+20x+23}, \ \psi_2(x,y) = \frac{72y/h}{2x^2+20x+23}.$$

The fact

$$\psi_1'(x) = \frac{8(2x^2-16x-103)}{(2x^2+20x+23)^2} < 0,$$

$$\phi_2'(x) = \frac{18(34x^2+97x+94)}{(2x^2+20x+23)^2} > 0,$$

for $x \in [-1,1]$ means that $\psi_1(x)$ and $\phi_2(x)$ are monotonously decreasing and monotonously increasing on $[-1,1]$, respectively, thus

$$\frac{8}{15} = \psi_1(1) \leqslant \psi_1\big(\cos(\rho h)\big) \leqslant \psi_1(-1) = 8, \tag{2.27}$$

$$-\frac{48}{5} = \phi_2(-1) \leqslant \phi_2\big(\cos(\rho h)\big) \leqslant \phi_2(1) = 0. \tag{2.28}$$

Meanwhile, we recognize that

$$\frac{4}{5} \leqslant \varphi_2\big(\cos(\rho h)\big) \leqslant 2 - \frac{1}{3}\sqrt{\frac{10}{3}} < 2, \tag{2.29}$$

$$|\psi_2\Big(\cos(\rho h), \sin(\rho h)\Big)| \leqslant \frac{6}{h}, \tag{2.30}$$

which can be shown by some simple calculation. In addition, noticing $5 \leqslant 2x^2+20x+23 \leqslant 45$ for $x \in [-1, 1]$, we have

$$\Big|\varphi_1\Big(\cos(\rho h), \sin(\rho h)\Big)\Big| \leqslant \frac{4}{5}h. \tag{2.31}$$

In addition, from (2.17), we conclude

$$\frac{\tau^{-\gamma}}{\Gamma(2-\gamma)}\Big[a_k - \sum_{l=1}^{k-1}(\lambda_{k-l-1}^{(\gamma)} - \lambda_{k-l}^{(\gamma)})a_l - \lambda_{k-1}^{(\gamma)}a_0\Big] = \kappa_1 c_k - \kappa_2 b_k + p_k, \quad 1 \leqslant k \leqslant N. \tag{2.32}$$

Denote $\mu = \tau^\gamma \Gamma(2-\gamma)$. The substitution of (2.25) and (2.26) into (2.32) leads to

$$\begin{aligned}
&\Big[1 - \kappa_1\phi_2\big(\cos(\rho h)\big)\frac{\mu}{h^2} + \mathbf{i}\kappa_2\phi_1\big(\cos(\rho h), \sin(\rho h)\big)\frac{\mu}{h}\Big]a_k \\
=&\sum_{l=1}^{k-1}(\lambda_{k-l-1}^{(\gamma)} - \lambda_{k-l}^{(\gamma)})a_l + \lambda_{k-1}^{(\gamma)}a_0 + \mu p_k + \mu\Big[\kappa_1\varphi_2\Big(\cos(\rho h)\Big) - \mathbf{i}\kappa_2\varphi_1\Big(\cos(\rho h), \sin(\rho h)\Big)\Big]r_k \\
&- \mu\Big[\kappa_2\psi_1\Big(\cos(\rho h)\Big) + \mathbf{i}\kappa_1\psi_2\Big(\cos(\rho h), \sin(\rho h)\Big)\Big]q_k, \quad 1 \leqslant k \leqslant N.
\end{aligned} \tag{2.33}$$

By (2.28), it is easily resulted that

$$\Big|1 - \kappa_1\phi_2\big(\cos(\rho h)\big)\frac{\mu}{h^2} + \mathbf{i}\kappa_2\phi_1\big(\cos(\rho h), \sin(\rho h)\big)\frac{\mu}{h}\Big| \geqslant 1$$

and hence Eq. (2.33) can be evaluated as

$$\begin{aligned}
|a_k| \leqslant &\sum_{l=1}^{k-1}(\lambda_{k-l-1}^{(\gamma)} - \lambda_{k-l}^{(\gamma)})|a_l| + \lambda_{k-1}^{(\gamma)}|a_0| \\
&+ \mu|p_k| + \mu\Big|\kappa_1\varphi_2\Big(\cos(\rho h)\Big) - \mathbf{i}\kappa_2\varphi_1\Big(\cos(\rho h), \sin(\rho h)\Big)\Big||r_k| \\
&+ \mu\Big|\kappa_2\psi_1\Big(\cos(\rho h)\Big) + \mathbf{i}\kappa_1\psi_2\Big(\cos(\rho h), \sin(\rho h)\Big)\Big||q_k|, \quad 1 \leqslant k \leqslant N.
\end{aligned} \tag{2.34}$$

The usage of $\mu = \tau^\gamma\Gamma(2-\gamma) = (k\tau)^\gamma\Gamma(1-\gamma)k^{-\gamma}(1-\gamma) < T^\gamma\Gamma(1-\gamma)\lambda_{k-1}^{(\gamma)}$ into the above inequality gives

$$|a_k| \leqslant \sum_{l=1}^{k-1}(\lambda_{k-l-1}^{(\gamma)} - \lambda_{k-l}^{(\gamma)})|a_l| + \lambda_{k-1}^{(\gamma)}\Psi_k, \tag{2.35}$$

with

$$\begin{aligned}\Psi_k =&|a_0| + T^\gamma\Gamma(1-\gamma)\Big[|p_k| + \Big|\kappa_1\varphi_2\Big(\cos(\rho h)\Big) - \mathbf{i}\kappa_2\varphi_1\Big(\cos(\rho h), \sin(\rho h)\Big)\Big||r_k| \\ &+ \Big|\kappa_2\psi_1\Big(\cos(\rho h)\Big) + \mathbf{i}\kappa_1\psi_2\Big(\cos(\rho h), \sin(\rho h)\Big)\Big||q_k|\Big],\ 1 \leqslant k \leqslant N.\end{aligned}$$

Taking the square on both sides of the inequality (2.35), by Cauchy-Schwarz inequality, we get

$$|a_k|^2 \leqslant \sum_{l=1}^{k-1} (\lambda_{k-l-1}^{(\gamma)} - \lambda_{k-l}^{(\gamma)})|a_l|^2 + \lambda_{k-1}^{(\gamma)}\Psi_k^2,\ 1 \leqslant k \leqslant N. \tag{2.36}$$

Noting that

$$\begin{aligned}\Psi_k^2 \leqslant&2|a_0|^2 + 6T^{2\gamma}\Gamma^2(1-\gamma)\Big\{|p_k|^2 + \Big[\kappa_1^2\varphi_2^2\Big(\cos(\rho h)\Big) + \kappa_2^2\varphi_1^2\Big(\cos(\rho h), \sin(\rho h)\Big)\Big]|r_k|^2 \\ &+ \Big[\kappa_2^2\psi_1^2\Big(\cos(\rho h)\Big) + \kappa_1^2\psi_2^2\Big(\cos(\rho h), \sin(\rho h)\Big)\Big]|q_k|^2\Big\},\end{aligned}$$

it follows from (2.36) that

$$\|u^k\|^2 \leqslant \sum_{l=1}^{k-1} (\lambda_{k-l-1}^{(\gamma)} - \lambda_{k-l}^{(\gamma)})\|u^l\|^2 + \lambda_{k-1}^{(\gamma)}\Phi,\ 1 \leqslant k \leqslant N. \tag{2.37}$$

where

$$\begin{aligned}\Phi =&2\|u^0\|^2 + 6T^{2\gamma}\Gamma^2(1-\gamma)\max_{1\leqslant l\leqslant N}\Big\{\|f^l\|^2 + \Big[\kappa_1^2\varphi_2^2\Big(\cos(\rho h)\Big) + \kappa_2^2\varphi_1^2\Big(\cos(\rho h), \sin(\rho h)\Big)\Big]\|\widetilde{g}^l\|^2 \\ &+ \Big[\kappa_2^2\psi_1^2\Big(\cos(\rho h)\Big) + \kappa_1^2\psi_2^2\Big(\cos(\rho h), \sin(\rho h)\Big)\Big]\|g^l\|^2\Big\}.\end{aligned}$$

By the mathematical induction method, from (2.37), it is resulted that

$$\|u^k\|^2 \leqslant \Phi, \quad 1 \leqslant k \leqslant N. \tag{2.38}$$

Further, by (2.27), (2.29)–(2.31), it produces

$$\begin{aligned}\kappa_1^2\varphi_2^2\Big(\cos(\rho h)\Big) + \kappa_2^2\varphi_1^2\Big(\cos(\rho h), \sin(\rho h)\Big) \leqslant 4\kappa_1^2 + 16\kappa_2^2h^2/25, \\ \kappa_2^2\psi_1^2\Big(\cos(\rho h)\Big) + \kappa_1^2\psi_2^2\Big(\cos(\rho h), \sin(\rho h)\Big) \leqslant 64\kappa_2^2 + 36\kappa_1^2/h^2.\end{aligned}$$

The conclusion holds from (2.38) and the above inequalities. The proof ends. □

In the following, the stability and convergence of the difference scheme (2.13)–(2.16) will be discussed.

Theorem 2. *(Stability) The difference scheme* (2.13)–(2.16) *is unconditionally stable with respect to the initial values.*

Proof. Suppose $\widetilde{\theta}_j^k$, $(\widetilde{\theta_x})_j^k$ and $(\widetilde{\theta}_{xx})_j^k$ are approximations of the solutions $\theta_j^k, (\theta_x)_j^k$ and $(\theta_{xx})_j^k$ of the difference scheme (2.13)–(2.16) with the initial values $u_0(x) + \xi(x)$, where $\xi(x)$ is a perturbation term, respectively. Denote $u_j^k = \theta_j^k - \widetilde{\theta}_j^k$, $v_j^k = (\theta_x)_j^k - (\widetilde{\theta_x})_j^k$ and $w_j^k = (\theta_{xx})_j^k - (\widetilde{\theta}_{xx})_j^k$. Then it holds

$$D_t^\gamma u_j^k = \kappa_1 w_j^k - \kappa_2 v_j^k, \quad 1 \leqslant j \leqslant M,\ 1 \leqslant k \leqslant N, \tag{2.39}$$

$$\frac{7}{16}\Big(v_{j+1}^k + v_{j-1}^k\Big) + v_j^k - \frac{h}{16}\Big(w_{j+1}^k - w_{j-1}^k\Big) = \frac{15}{16h}(u_{j+1}^k - u_{j-1}^k),$$
$$1 \leqslant j \leqslant M,\ 1 \leqslant k \leqslant N, \tag{2.40}$$

$$\frac{9}{8h}\Big(v_{j+1}^k - v_{j-1}^k\Big) - \frac{1}{8}\Big(w_{j+1}^k + w_{j-1}^k\Big) + w_j^k = \frac{3}{h^2}(u_{j+1}^k - 2u_j^k + u_{j-1}^k),$$
$$1 \leqslant j \leqslant M,\ 1 \leqslant k \leqslant N, \tag{2.41}$$

$$u_j^0 = \xi(x_j), \quad 1 \leqslant j \leqslant M. \tag{2.42}$$

Similar to the process of the prior estimate, we have

$$\|u^k\| \leqslant \|u^0\|, \quad 1 \leqslant k \leqslant N. \tag{2.43}$$

□

Let

$$e_j^k = \Theta_j^k - \theta_j^k,\ \varepsilon_j^k = (\Theta_x)_j^k - (\theta_x)_j^k,\ \eta_j^k = (\Theta_{xx})_j^k - (\theta_{xx})_j^k,\ 1 \leqslant j \leqslant M, 0 \leqslant k \leqslant N.$$

The error system is obtained by the substraction of (2.13)–(2.16) from (2.8)–(2.11) in the form of

$$D_t^\gamma e_j^k = \kappa_1 \eta_j^k - \kappa_2 \varepsilon_j^k + R_j^k, \quad 1 \leqslant j \leqslant M,\ 1 \leqslant k \leqslant N, \tag{2.44}$$

$$\frac{7}{16}\Big(\varepsilon_{j+1}^k + \varepsilon_{j-1}^k\Big) + \varepsilon_j^k - \frac{h}{16}\Big(\eta_{j+1}^k - \eta_{j-1}^k\Big) = \frac{15}{16h}(e_{j+1}^k - e_{j-1}^k) + S_j^k,$$
$$1 \leqslant j \leqslant M,\ 1 \leqslant k \leqslant N, \tag{2.45}$$

$$\frac{9}{8h}\Big(\varepsilon_{j+1}^k - \varepsilon_{j-1}^k\Big) - \frac{1}{8}\Big(\eta_{j+1}^k + \eta_{j-1}^k\Big) + \eta_j^k = \frac{3}{h^2}(e_{j+1}^k - 2e_j^k + e_{j-1}^k) + T_j^k,$$
$$1 \leqslant j \leqslant M,\ 1 \leqslant k \leqslant N, \tag{2.46}$$

$$e_j^0 = 0, \quad 1 \leqslant j \leqslant M. \tag{2.47}$$

Noticing (2.12), a straightforward application of Theorem 1 to (2.44)–(2.47) yields

$$\begin{aligned}\|e^k\|^2 &\leqslant 6T^{2\gamma}\Gamma^2(1-\gamma)\max_{1\leqslant l\leqslant N}\Big[\|R^l\|^2 + (4\kappa_1^2 + 16\kappa_2^2h^2/25)\|T^l\|^2 + (64\kappa_2^2 + 36\kappa_1^2/h^2)\|S^l\|^2\Big] \\ &\leqslant 6T^{2\gamma}\Gamma^2(1-\gamma)Lc^2\Big[(\tau^{2-\gamma})^2 + 4(\kappa_1^2 + 16\kappa_2^2)(h^6)^2 + 16\kappa_2^2(h^7)^2/25 + 36\kappa_1^2(h^5)^2\Big], \\ &\qquad 1 \leqslant k \leqslant N.\end{aligned}$$

Further, it follows

$$\|e^k\| \leqslant \sqrt{6L}T^{\gamma}\Gamma(1-\gamma)c\Big(\tau^{2-\gamma} + 2\sqrt{\kappa_1^2 + 16\kappa_2^2}h^6 + 4\kappa_2 h^7/5 + 6\kappa_1 h^5\Big), \quad 1 \leqslant k \leqslant N. \tag{2.48}$$

Therefore, the following theorem holds.

Theorem 3. *(Convergence) Suppose* $\theta(x,t) \in C^{8,2}(\Omega)$. *The difference scheme* (2.13)–(2.16) *is unconditionally convergent; namely, it holds*

$$\|e^k\| \leqslant \sqrt{6L}T^{\gamma}\Gamma(1-\gamma)c\Big(\tau^{2-\gamma} + 2\sqrt{\kappa_1^2 + 16\kappa_2^2}h^6 + 4\kappa_2 h^7/5 + 6\kappa_1 h^5\Big), \quad 1 \leqslant k \leqslant N.$$

From Theorem 3, the global spatial fifth-order accuracy and temporal $(2-\gamma)$th-order accuracy of the proposed method are theoretically concluded. However, from the numerical results, the global one order higher accuracy of the method in space can achieved for solving the problem subjected to the PBCs.

3. Extensions to the variable coefficient TFADEs

The ideas of dealing with the constant coefficient TFADEs (2.1)–(2.3) can be extended to treat the variable coefficient problems subject to three different kinds of boundary conditions: PBCs, Dirichlet boundary conditions (DBCs), and NBCs, respectively.

3.1. Periodic boundary problem

Consider the variable coefficient time-fractional advection-diffusion problem

$$ {}_0^C\mathcal{D}_t^{\gamma}\theta(x,t) = a(x,t)\theta_{xx}(x,t) - b(x,t)\theta_x(x,t) + f(x,t), \quad x \in \mathbb{R},\ t \in (0,T], \tag{3.1}$$

$$\theta(x,0) = \theta_0(x), \quad x \in \mathbb{R}, \tag{3.2}$$

$$\theta(x,t) = \theta(x+L,t), \quad x \in \mathbb{R},\ t \in [0,T], \tag{3.3}$$

where $L > 0, a(x,t) > 0$ for any $x \in \mathbb{R}$ and $t \in (0,T]$.

Similar to the process of constructing difference scheme (2.13)–(2.16) for the constant coefficient problem (2.1)–(2.3) on a domain $\Omega = [0,L] \times [0,T]$ with the space length of a period, a high-order CCD scheme for solving the problem (3.1)–(3.3) on Ω can be obtained in the form of

$$D_t^{\gamma}\theta_j^k = a(x_j,t_k)(\theta_{xx})_j^k - b(x_j,t_k)(\theta_x)_j^k + f_j^k, \quad 1 \leqslant j \leqslant M,\ 1 \leqslant k \leqslant N, \tag{3.4}$$

$$\frac{7}{16}[(\theta_x)_{j+1}^k + (\theta_x)_{j-1}^k] + (\theta_x)_j^k - \frac{h}{16}[(\theta_{xx})_{j+1}^k - (\theta_{xx})_{j-1}^k] = \frac{15}{16h}(\theta_{j+1}^k - \theta_{j-1}^k),$$
$$1 \leqslant j \leqslant M,\ 1 \leqslant k \leqslant N, \tag{3.5}$$

$$\frac{9}{8h}[(\theta_x)_{j+1}^k - (\theta_x)_{j-1}^k] - \frac{1}{8}[(\theta_{xx})_{j+1}^k + (\theta_{xx})_{j-1}^k] + (\theta_{xx})_j^k = \frac{3}{h^2}(\theta_{j+1}^k - 2\theta_j^k + \theta_{j-1}^k),$$
$$1 \leqslant j \leqslant M,\ 1 \leqslant k \leqslant N, \tag{3.6}$$

$$\theta_j^0 = \theta_0(x_j), \quad 1 \leqslant j \leqslant M. \tag{3.7}$$

At each time level $t = t_k$ $(1 \leqslant k \leqslant N)$, the difference scheme (3.4)–(3.7) is a linear algebraic system with respect to the unknowns $[\theta^{\mathbf{k}}_{\mathbf{x}}, \theta^{\mathbf{k}}_{\mathbf{xx}}, \theta^{\mathbf{k}}]^T$. The local truncation errors are of order $\mathcal{O}(h^6 + \tau^{2-\gamma})$. The system can be solved by the algorithm described in section 2.1.

3.2. Dirichlet and Neumann boundary problem

Consider the variable coefficient time-fractional advection-diffusion problem

$$
\begin{aligned}
&{}_0^C\mathcal{D}_t^{\gamma}\theta(x,t) = a(x,t)\theta_{xx}(x,t) - b(x,t)\theta_x(x,t) + f(x,t), \quad x \in [0,L],\ t \in (0,T], && (3.8)\\
&\theta(x,0) = \theta_0(x), \quad x \in [0,L], && (3.9)\\
&d_1(x)\theta_x(x,t) + d_0(x)\theta(x,t) = c(x,t), \quad x = 0, L,\ t \in (0,T], && (3.10)
\end{aligned}
$$

where $a(x,t) > 0$ for any $x \in [0,L]$ and $t \in (0,T]$.

When $d_1(x) = 0, d_0(x) = 1$, Eq. (3.10) is the DBCs; while if $d_1(x) = 1, d_0(x) = 0$, it is the NBCs.

When a CCD scheme for problem (3.8)–(3.10) is attempted to be established, the major point different from the problem (3.1)–(3.3) lies in that some special attentions must be paid on the handling of boundary conditions. The numbers of total unknowns are $3(M+1)$ if the idea of CCD scheme is used for solving (3.8)–(3.10). Equation (3.8) can be considered at all space mesh points $x_j (0 \leqslant j \leqslant M)$, however, the relationship (2.6)–(2.7) are only meaningful for the interior nodes $x_j (1 \leqslant j \leqslant M-1)$. Combining two boundary conditions (3.10), additional two conditions are needed to complete the system. For this purpose, for both the left and right boundary, the following two expressions with dominated truncation terms of order five are introduced as below [30].

$$14(\Theta_x)_0^k + 16(\Theta_x)_1^k + 2h(\Theta_{xx})_0^k - 4h(\Theta_{xx})_1^k + \frac{1}{h}(31\Theta_0^k - 32\Theta_1^k + \Theta_2^k) = \mathcal{O}(h^5), \tag{3.11}$$

$$14(\Theta_x)_M^k + 16(\Theta_x)_{M-1}^k - 2h(\Theta_{xx})_M^k + 4h(\Theta_{xx})_{M-1}^k - \frac{1}{h}(31\Theta_M^k - 32\Theta_{M-1}^k + \Theta_{M-2}^k) = \mathcal{O}(h^5). \tag{3.12}$$

Hence, considering Eq. (3.8) at all space mesh points, noticing (2.6)–(2.7), (3.11)–(3.12) and initial-boundary value conditions (3.9)–(3.10), a high-order CCD scheme for solving the

problem (3.8)-(3.10) can be produced as follows:

$$D_t^{\gamma}\theta_j^k = a(x_j,t_k)(\theta_{xx})_j^k - b(x_j,t_k)(\theta_x)_j^k + f_j^k, \quad 0 \leqslant j \leqslant M,\ 1 \leqslant k \leqslant N, \tag{3.13}$$

$$14(\theta_x)_0^k + 16(\theta_x)_1^k + 2h(\theta_{xx})_0^k - 4h(\theta_{xx})_1^k + \frac{1}{h}(31\theta_0^k - 32\theta_1^k + \theta_2^k) = 0, \quad 1 \leqslant k \leqslant N, \tag{3.14}$$

$$\frac{7}{16}[(\theta_x)_{j+1}^k + (\theta_x)_{j-1}^k] + (\theta_x)_j^k - \frac{h}{16}[(\theta_{xx})_{j+1}^k - (\theta_{xx})_{j-1}^k] = \frac{15}{16h}(\theta_{j+1}^k - \theta_{j-1}^k),$$
$$1 \leqslant j \leqslant M-1,\ 1 \leqslant k \leqslant N, \tag{3.15}$$

$$14(\theta_x)_M^k + 16(\theta_x)_{M-1}^k - 2h(\theta_{xx})_M^k + 4h(\theta_{xx})_{M-1}^k - \frac{1}{h}(31\theta_M^k - 32\theta_{M-1}^k + \theta_{M-2}^k) = 0,$$
$$1 \leqslant k \leqslant N, \tag{3.16}$$

$$\frac{9}{8h}[(\theta_x)_{j+1}^k - (\theta_x)_{j-1}^k] - \frac{1}{8}[(\theta_{xx})_{j+1}^k + (\theta_{xx})_{j-1}^k] + (\theta_{xx})_j^k = \frac{3}{h^2}(\theta_{j+1}^k - 2\theta_j^k + \theta_{j-1}^k),$$
$$1 \leqslant j \leqslant M-1,\ 1 \leqslant k \leqslant N, \tag{3.17}$$

$$d_1(x_j)(\theta_x)_j^k + d_0(x_j)\theta_j^k = c(x_j,t_k),\ j = 0, M,\ 1 \leqslant k \leqslant N, \tag{3.18}$$

$$\theta_j^0 = \theta_0(x_j), \quad 0 \leqslant j \leqslant M. \tag{3.19}$$

At each time level $t = t_k$ ($1 \leqslant k \leqslant N$), the difference scheme (3.13)–(3.19) is a linear algebraic system with respect to the unknowns $[\theta_{\mathbf{x}}^{\mathbf{k}}, \theta_{\mathbf{xx}}^{\mathbf{k}}, \theta^{\mathbf{k}}]^T$ with $\theta_{\mathbf{x}}^{\mathbf{k}} = [(\theta_x)_0^k, (\theta_x)_1^k, \ldots, (\theta_x)_M^k]$, $\theta_{\mathbf{xx}}^{\mathbf{k}} = [(\theta_{xx})_0^k, (\theta_{xx})_1^k, \ldots, (\theta_{xx})_M^k]$ and $\theta^{\mathbf{k}} = [\theta_0^k, \theta_1^k, \ldots, \theta_M^k]$. If the sequence of equations in the difference scheme (3.13)–(3.19) is arranged in the order that, firstly, Eqs. (3.13) and (3.18) for $j = 0$ and (3.14); secondly, Eqs. (3.13), (3.15) and (3.17) for $j = 1$; thirdly, Eqs. (3.13), (3.15) and (3.17) for $j = 2$; it proceeds in this way until Eqs. (3.13), (3.15) and (3.17) for $j = M-1$; finally, Eqs. (3.13) and (3.18) for $j = M$ and (3.16). The coefficient matrix of this system owns a triple-tridiagonal structure and can be solved in two steps: triple-forward elimination and triple-backward substitution; see [30].

4. Numerical experiments

In this section, several examples are computed to demonstrate the numerical accuracy and computational efficiency of the CCD schemes we presented in the above work. The former three ones, are to solve the time-fractional advection-diffusion problems subject to the PBCs, where the former two ones are for the constant coefficient case which are used to confirm our theoretical analysis and the third one is for a variable coefficient case, which supports the wide application of the present scheme. Then the scheme (3.13)–(3.19) for solving the time-fractional advection-diffusion problems subject to the DBCs and NBCs is tested numerically by the last two examples. Though the rigorous theoretical analysis for the latter schemes is not available now, numerical computational results show the efficiency and the high-order accuracy of the present schemes.

Denote

$$E_{\infty}^{(p)}(h,\tau) = \max_{\substack{1\leqslant j\leqslant M\\ 0\leqslant k\leqslant N}} |\Theta_j^k - \theta_j^k|, \quad E_2^{(p)}(h,\tau) = \max_{0\leqslant k\leqslant N} \|\Theta^k - \theta^k\|,$$

$$rate_{2,\tau}^{(p)} = \log_2 \frac{E_2^{(p)}(h,\tau)}{E_2^{(p)}(h,\tau/2)}, \quad rate_{\infty,\tau}^{(p)} = \log_2 \frac{E_\infty^{(p)}(h,\tau)}{E_\infty^{(p)}(h,\tau/2)},$$

$$rate_{2,h}^{(p)} = \log_2 \frac{E_2^{(p)}(h,\tau)}{E_2^{(p)}(h/2,\tau)}, \quad rate_{\infty,h}^{(p)} = \log_2 \frac{E_\infty^{(p)}(h,\tau)}{E_\infty^{(p)}(h/2,\tau)}.$$

Example 1.(constant coefficients and zero initial value problem subject to the PBCs)

In (2.1)–(2.3), taking $\kappa_1 = \kappa_2 = 1$, $f(x,t) = t^3\Big\{\sin(x)\frac{\Gamma(4+\gamma)}{6} + [\sin(x)+\cos(x)]t^\gamma\Big\}$, $\theta_0(x) = 0$, $L = 2\pi$. The exact solution is $\theta(x,t) = \sin(x)t^{3+\gamma}$. On the domain $\Omega = [0,2\pi]\times[0,1]$, we compute the example using the difference scheme (2.13)–(2.16).

At first, the numerical accuracy in the temporal direction is verified. Table 1 lists some computational results and the convergence orders with a fixed spatial step size $h = \pi/5$ and different temporal step sizes τ. Because of the high-order accuracy in the spatial direction, when the values of τ are taken as 1/10, 1/20, 1/40, 1/80 and 1/160, respectively, a fixed value of $h = \pi/5$ can guarantee that the dominated errors of numerical results come from the approximation in the temporal direction. From the data of Table 1, the convergence order $2-\gamma$ of the difference scheme (2.13)–(2.16) in the temporal direction is confirmed.

Table 1: The L^2 norm errors and convergence orders of difference scheme (2.13)–(2.16) in the temporal direction with a fixed $h = \pi/5$.

τ	$\gamma = 0.5$		$\gamma = 0.75$	
	$E_2^{(p)}(h,\tau)$	$rate_{2,\tau}^{(p)}$	$E_2^{(p)}(h,\tau)$	$rate_{2,\tau}^{(p)}$
1/10	3.624786×10^{-2}	1.41	1.085285×10^{-1}	1.19
1/20	1.366049×10^{-2}	1.44	4.741326×10^{-2}	1.22
1/40	5.030519×10^{-3}	1.46	2.039462×10^{-2}	1.23
1/80	1.822909×10^{-3}	1.49	8.688707×10^{-3}	1.24
1/160	6.508657×10^{-4}	—	3.678657×10^{-3}	—

Then, for $\gamma = 0.5$, with a sufficiently small $\tau = 1/200,000$ and varying space mesh step size h, the computational errors and convergence orders in the spatial direction in the sense of discrete L^2 norm and the maximum norm are reported in Table 2, respectively. The conclusion of the sixth-order convergence of the difference scheme (2.13)–(2.16) in space can be drawn from the numerical results in Table 2, which is one-order higher than the theoretical analysis accuracy in space illustrated in section 2.2.

Finally, with the analytical solution $\theta(x,t) = \sin(x)t^{3+\gamma}$, the computational efficiency of the difference scheme (2.13)–(2.16) for a fixed $\kappa_2 = 1$ and varying $\kappa_1 = 1, 0.1, 0.01, \ldots, 10^{-10}$ will be tested on the domain $[0,2\pi]\times[0,1]$. The problem becomes more and more advection-dominated as κ_1 decreases gradually. For the purpose of illustrate the advantages of the difference scheme (2.13)–(2.16) over the fourth-order compact difference algorithm proposed by Mohebbi and Abbaszadeh in [23] subject to the PBCs, Table 3 shows the corresponding

Table 2: Errors and convergence orders of difference scheme (2.13)–(2.16) in the spatial direction with $\tau = 1/200,000$ and $\gamma = 0.5$.

M	$E_2^{(p)}(h,\tau)$	$rate_{2,h}^{(p)}$	$E_\infty^{(p)}(h,\tau)$	$rate_{\infty,h}^{(p)}$
4	3.158216×10^{-3}	6.36	1.489712×10^{-3}	6.10
8	3.847547×10^{-5}	6.12	2.170617×10^{-5}	6.12
16	5.545114×10^{-7}	6.14	3.124685×10^{-7}	6.14
32	7.840538×10^{-9}	—	4.423542×10^{-9}	—

numerical results for these two classes of difference schemes with $\tau = 1/2000, h = \pi/10$ and $\gamma = 0.5$. From Table 3, we find that for this example, the difference scheme (2.13)–(2.16) is not quite sensitive as the advection term is gradually dominated, while the computational efficiency of the algorithm in [23] is more or less influenced. Computational results of the latter one are inferior to the present one and the numerical errors are polluted when κ_1 varies from 1 to 0.1 and from 0.1 to 0.01.

Table 3: The L^2 norm errors of difference scheme (2.13)–(2.16) and the algorithm in [23] with the fixed $\kappa_2 = 1, \tau = 1/2000, h = \pi/10$ and $\gamma = 0.5$.

	difference scheme (2.13) – –(2.16)	the algorithm in [23]
κ_1	$E_2^{(p)}(h,\tau)$	$E_2^{(p)}(h,\tau)$
1	1.526080×10^{-5}	7.008885×10^{-5}
10^{-1}	2.210722×10^{-5}	4.993898×10^{-4}
10^{-2}	2.308840×10^{-5}	4.095970×10^{-3}
10^{-3}	2.319064×10^{-5}	6.693160×10^{-3}
10^{-4}	2.320090×10^{-5}	6.779515×10^{-3}
10^{-5}	2.320194×10^{-5}	6.783483×10^{-3}
10^{-6}	2.320204×10^{-5}	6.783831×10^{-3}
10^{-7}	2.320265×10^{-5}	6.783866×10^{-3}
10^{-8}	2.320155×10^{-5}	6.783869×10^{-3}
10^{-9}	2.318934×10^{-5}	6.783870×10^{-3}
10^{-10}	2.356975×10^{-5}	6.783870×10^{-3}

In addition, with $\kappa_1 = \kappa_2 = 1$, $\gamma = 0.5$ and $T = 1$, Table 4 reports the computational errors in L^2 norm and the consuming CPU time on the same machine of the difference scheme (2.13)–(2.16) and the scheme in [23] for computing this example, where the optimal step size ratios are taken, namely, $\tau^{1.5} \approx h^6$ for the scheme (2.13)–(2.16) and $\tau^{1.5} \approx h^4$ for the scheme in [23]. By comparison, one can find that in same or almost same computational errors, the present CCD scheme spends less CPU time than the method in [23]. The efficiency of the proposed CCD method can be read off.

Table 4: Comparison in the L^2 norm errors and CPU time of difference scheme (2.13)–(2.16) and the algorithm in [23] with $\kappa_1 = \kappa_2 = 1, T = 1$ and $\gamma = 0.5$.

N	difference scheme (2.13)–(2.16)			the algorithm in [23]		
	M	$E_2^{(p)}(h,\tau)$	CPU time (s)	M	$E_2^{(p)}(h,\tau)$	CPU time (s)
100	20	1.319789×10^{-3}	0.07	35	1.322789×10^{-3}	0.23
200	24	4.744210×10^{-4}	0.18	46	4.751297×10^{-4}	0.64
400	28	1.696485×10^{-4}	0.48	59	1.697895×10^{-4}	1.77
800	33	6.045262×10^{-5}	1.33	77	6.047490×10^{-5}	5.63
1600	40	2.149065×10^{-5}	4.62	100	2.149023×10^{-5}	19.47
3200	47	7.627122×10^{-6}	16.82	130	7.624860×10^{-6}	77.16
6400	56	2.703833×10^{-6}	69.28	168	2.702363×10^{-6}	335.12

Example 2.(constant coefficients and non-zero initial value problem subject to the PBCs) In (2.1)–(2.3), taking

$$\theta_0(x) = \sin(x), L = 2\pi, f(x,t) = 2\sin(x)t^{1-\gamma}E_{1,2-\gamma}(2t) + \exp(2t)[\kappa_1 \sin(x) + \kappa_2 \cos(x)],$$

where $E_{\mu,\nu}(z)$ is the Mittag-Leffler function with two parameters, which is defined by

$$E_{\mu,\nu}(z) = \sum_{n=0}^{\infty} \frac{z^n}{\Gamma(\mu n + \nu)}.$$

The exact solution of *Example 2* is $\theta(x,t) = \sin(x)\exp(2t)$.

Firstly, we demonstrate the numerical accuracy of the difference scheme (2.13)–(2.16) in the temporal and the spatial directions by computing this example with $\kappa_1 = \kappa_2 = 1$. With a fixed spatial step size $h = \pi/10$ and varying temporal step sizes τ, the example is computed using the proposed scheme (2.13)–(2.16). The numerical results are displayed in Table 4, from which, we observe that the $(2-\gamma)$th order convergence of the difference scheme (2.13)–(2.16) in temporal direction is achieved.

Then, we numerically compute the example by the proposed scheme (2.13)–(2.16) with different spatial step sizes. The absolute errors and convergence orders in the discrete L^2 norm and the discrete maximum norm are contained in Table 6 simultaneously. From the table, it is clear that the numerical convergence order in the spatial direction for this non-zero initial value problem still keeps as six.

In addition, with different parameter values κ_1 and κ_2, we would like to compare the computational effectiveness between the difference scheme (2.13)–(2.16) and the algorithm by Mohebbi and Abbaszadeh in [23] subject to the PBCs for this example. The similar phenomenon can be observed from the computational results shown in Table 7. In other words, the present numerical scheme is more robust than that in [23] for the example.

Example 3. (Problem with variable coefficients and PBCs)

Table 5: The L^2 norm errors and convergence orders of difference scheme (2.13)–(2.16) in the temporal direction with the fixed $h = \pi/10$ and $\kappa_1 = \kappa_2 = 1$.

τ	$\gamma = 0.5$		$\gamma = 0.75$	
	$E_2^{(p)}(h,\tau)$	$rate_{2,\tau}^{(p)}$	$E_2^{(p)}(h,\tau)$	$rate_{2,\tau}^{(p)}$
1/20	4.562697×10^{-2}	1.44	1.433820×10^{-1}	1.22
1/40	1.682598×10^{-2}	1.46	6.153342×10^{-2}	1.23
1/80	6.118270×10^{-3}	1.47	2.618919×10^{-2}	1.24
1/160	2.204032×10^{-3}	1.48	1.109067×10^{-2}	1.24
1/320	7.886979×10^{-4}	1.49	4.682418×10^{-3}	1.25
1/640	2.805887×10^{-4}	1.50	1.973047×10^{-3}	1.25
1/1280	9.904681×10^{-5}	—	8.301585×10^{-4}	—

Table 6: Errors and convergence orders of difference scheme (2.13)–(2.16) in the spatial direction with $\tau = 1/200,000$ for $\gamma = 0.5$ and $\kappa_1 = \kappa_2 = 1$.

M	$E_2^{(p)}(h,\tau)$	$rate_{2,h}^{(p)}$	$E_\infty^{(p)}(h,\tau)$	$rate_{\infty,h}^{(p)}$
4	2.805157×10^{-2}	6.36	1.381235×10^{-2}	6.16
8	3.418494×10^{-4}	6.09	1.925192×10^{-4}	6.09
16	5.007673×10^{-6}	7.11	2.824899×10^{-6}	7.11
32	3.631389×10^{-8}	—	2.048741×10^{-8}	—

Table 7: The L^2 norm errors of difference scheme (2.13)–(2.16) and the algorithm in [23] with the fixed $\kappa_2 = 1, \tau = 1/2000, h = \pi/10$ and $\gamma = 0.5$.

	difference scheme (2.13) – (2.16)	the algorithm in [23]
κ_1	$E_2^{(p)}(h,\tau)$	$E_2^{(p)}(h,\tau)$
1	5.027737×10^{-5}	6.394149×10^{-4}
10^{-1}	7.398945×10^{-5}	4.892821×10^{-3}
10^{-2}	7.739798×10^{-5}	3.904305×10^{-2}
10^{-3}	7.775318×10^{-5}	6.338290×10^{-2}
10^{-4}	7.778885×10^{-5}	6.423751×10^{-2}
10^{-5}	7.779245×10^{-5}	6.427997×10^{-2}
10^{-6}	7.779281×10^{-5}	6.428377×10^{-2}
10^{-7}	7.779860×10^{-5}	6.428414×10^{-2}
10^{-8}	7.779933×10^{-5}	6.428418×10^{-2}
10^{-9}	7.770414×10^{-5}	6.428419×10^{-2}
10^{-10}	8.282759×10^{-5}	6.428419×10^{-2}

In (3.1)–(3.3), taking $a(x,t) = x+1$, $b(x,t) = t\sin(x)$, $f(x,t) = t^3\Big\{\cos(x)\Big[\frac{\Gamma(4+\gamma)}{6} + (x+1)t^{\gamma}\Big] - \sin^2(x)t^{1+\gamma}\Big\}$, $L = 2\pi$ and $\theta_0(x) = 0$. The exact solution is $\theta(x,t) = \cos(x)t^{3+\gamma}$.

On a space periodic domain $[0, 2\pi] \times [0, 1]$, the numerical solution is computed using the difference scheme (3.4)–(3.7). Firstly, with a fixed value $M = 40$, the problem is numerically computed to test the computational errors and numerical accuracy in the temporal direction. The data of Table 8 indicates that the numerical accuracy in the temporal direction of the difference scheme (3.4)–(3.7) can also achieve $2 - \gamma$.

Table 8: The maximum errors and convergence orders of difference scheme (3.4)–(3.7) in time with a fixed $h = \pi/20$.

τ	$\gamma = 0.5$		$\gamma = 0.75$	
	$E_{\infty}^{(p)}(h,\tau)$	$rate_{\infty,\tau}^{(p)}$	$E_{\infty}^{(p)}(h,\tau)$	$rate_{\infty,\tau}^{(p)}$
1/10	1.760955×10^{-2}	1.41	5.051485×10^{-2}	1.20
1/20	6.617384×10^{-3}	1.44	2.193374×10^{-2}	1.22
1/40	2.437116×10^{-3}	1.46	9.410352×10^{-3}	1.23
1/80	8.857283×10^{-4}	1.47	4.006018×10^{-3}	1.24
1/160	3.190824×10^{-4}	1.48	1.697030×10^{-3}	1.24
1/320	1.142736×10^{-4}	1.49	7.167310×10^{-4}	1.25
1/640	4.076163×10^{-5}	1.49	3.021550×10^{-4}	1.25
1/1280	1.449935×10^{-5}	—	1.272410×10^{-4}	—

Fig. 1 plots the numerical solution by using the difference scheme (3.4)–(3.7) and the exact solution at $T = 5$ with different γ from 0.1 to 0.9 and $h = \pi/20, \tau = 1/200$. The close agreement of these two plots illustrates the efficiency of the difference scheme (3.4)–(3.7).

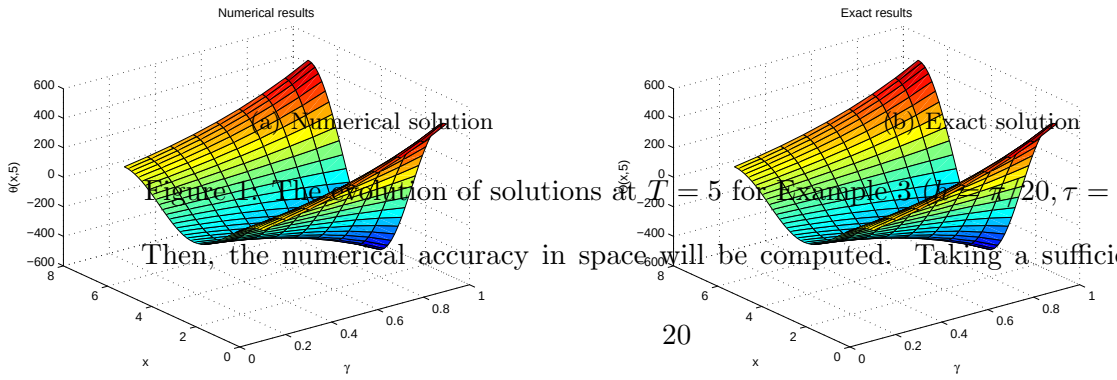

(a) Numerical solution (b) Exact solution

Figure 1: The evolution of solutions at $T = 5$ for Example 3 ($h = \pi/20, \tau = 1/200$).

Then, the numerical accuracy in space will be computed. Taking a sufficiently small

temporal step size $\tau = 1/200,000$, the numerical example is computed with different spatial step sizes $h = 2\pi/M$, $M = 4, 8, 16, 32$, respectively. When $\gamma = 0.5$, the discrete numerical errors and convergence orders are given in Table 9. Obviously, the convergence accuracy of the newly developed CCD scheme (3.4)–(3.7) in space also keeps to be sixth-order.

Table 9: Errors and convergence orders of difference scheme (3.4)–(3.7) in spatial direction with $\tau = 1/200,000$ and $\gamma = 0.5$.

M	$E_2^{(p)}(h,\tau)$	$rate_{2,h}^{(p)}$	$E_\infty^{(p)}(h,\tau)$	$rate_{\infty,h}^{(p)}$
4	7.959572×10^{-3}	6.54	5.333536×10^{-3}	6.52
8	8.550721×10^{-5}	6.24	5.811684×10^{-5}	6.30
16	1.132844×10^{-6}	7.20	7.391968×10^{-7}	7.23
32	7.728579×10^{-9}	—	4.927360×10^{-9}	—

Example 4.(Problem with DBCs)

In (3.8)–(3.10), taking $a(x,t) = 1$, $b(x,t) = 1$, $f(x,t) = \exp(-x)[\Gamma(3+\gamma)t^2/2 - 2(t^{2+\gamma} + 1)]$, $L = 2\pi$, $T = 1$, $d_1(x) \equiv 0$, $d_0(x) \equiv 1$, $c(0,t) = t^{2+\gamma} + 1, c(L,t) = \exp(-L)[t^{2+\gamma} + 1]$ and $\theta_0(x) = \exp(-x)$.

As a matter of fact, the problem is a one-dimensional time-fractional advection-diffusion case with Dirichlet boundary values. The exact solution is given by $\theta(x,t) = \exp(-x)[1 + t^{2+\gamma}]$.

The problem can also be computed using the fourth-order compact finite difference scheme presented in [23]. We find that, the approximation in time is by the same *L1* discretization for both the method in [23] and the newly proposed CCD scheme (3.13)–(3.19). The difference lies in the approximation in space. It is reported that the convergence order of the difference scheme in [23] is four in space, while our newly developed CCD scheme (3.13)–(3.19) can be expected to be much higher in space. To show this result, denote

$$E_\infty^{ND}(h,\tau) = \max_{\substack{0\leqslant j\leqslant M\\ 0\leqslant k\leqslant N}} |\Theta_j^k - \theta_j^k|,\ rate_{\infty,\tau}^{(ND)} = \log_2 \frac{E_\infty^{ND}(h,\tau)}{E_\infty^{ND}(h,\tau/2)},\ rate_{\infty,h}^{(ND)} = \log_2 \frac{E_\infty^{ND}(h,\tau)}{E_\infty^{ND}(h/2,\tau)}.$$

Firstly, the numerical convergence accuracy of the difference scheme (3.13)–(3.19) in time is verified. Taking a fixed $M = 40$ and different time step sizes, the computational results with different γ are put into Table 10. Apparently, the $(2-\gamma)$-th order numerical convergence in time is valid.

Secondly, for $\gamma = 0.5$, taking a sufficiently small $\tau = 1/200,000$ to ensure the dominated errors coming from the approximation of space derivatives, the higher-order numerical accuracy of the difference scheme (3.13)–(3.19) over the algorithm in [23] is illustrated in Table 11.

Finally, to further show the advantages of the difference scheme (3.13)–(3.19) over the algorithm in [23], for different anomalous diffusion parameters $\gamma = 0.25, 0.5, 0.75$, we plot the absolute error curves of the example at $T = 1$ under the same mesh size by using these

Table 10: The maximum errors and convergence orders of difference scheme (3.13)–(3.19) in time with a fixed $h = \pi/20$.

τ	$\gamma = 0.5$		$\gamma = 0.75$	
	$E_\infty^{ND}(h,\tau)$	$rate_{\infty,\tau}^{(ND)}$	$E_\infty^{ND}(h,\tau)$	$rate_{\infty,\tau}^{(ND)}$
10	4.222820×10^{-3}	1.44	1.420778×10^{-2}	1.21
20	1.558005×10^{-3}	1.46	6.138175×10^{-3}	1.23
40	5.665214×10^{-4}	1.47	2.621492×10^{-3}	1.24
80	2.041009×10^{-4}	1.48	1.112188×10^{-3}	1.24
160	7.307961×10^{-5}	1.49	4.700505×10^{-4}	1.25
320	2.604987×10^{-5}	1.49	1.982143×10^{-4}	1.25
640	9.248301×10^{-6}	1.50	8.346798×10^{-5}	1.25
1280	3.265004×10^{-6}	—	3.511203×10^{-5}	—

Table 11: Maximum errors and convergence orders of difference scheme (3.13)–(3.19) and the algorithm in [23] in the spatial direction with $\tau = 1/200,000$ and $\gamma = 0.5$.

τ	difference scheme (3.13)–(3.19)		the algorithm in [23]	
M	$E_\infty^{ND}(h,\tau)$	$rate_{\infty,h}^{(ND)}$	$E_\infty^{ND}(h,\tau)$	$rate_{\infty,h}^{(ND)}$
4	1.334236×10^{-2}	4.48	3.726883×10^{-2}	3.80
8	5.982602×10^{-4}	5.29	2.673271×10^{-3}	3.88
16	1.527300×10^{-5}	5.68	1.819528×10^{-4}	3.98
32	2.970387×10^{-7}	—	1.151053×10^{-5}	—

two classes of difference schemes, respectively. From the Fig. 2, we can recognize that the CCD scheme (3.13)–(3.19) is more accurate than the algorithm in [23].

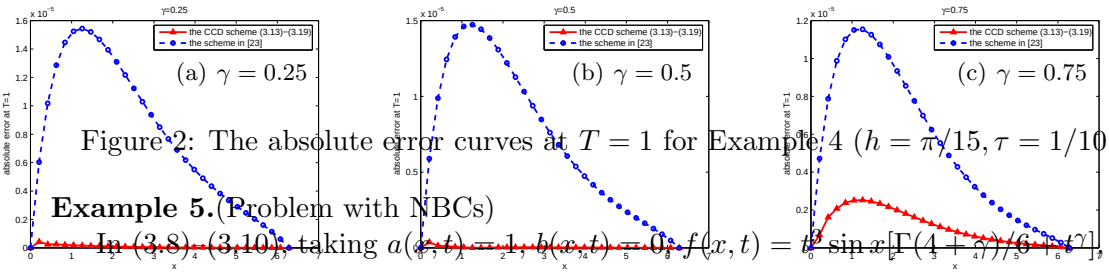

(a) $\gamma = 0.25$ (b) $\gamma = 0.5$ (c) $\gamma = 0.75$

Figure 2: The absolute error curves at $T = 1$ for Example 4 ($h = \pi/15, \tau = 1/10,000$).

Example 5. (Problem with NBCs)
In (3.8)–(3.10), taking $a(x,t) = 1$, $b(x,t) = 0$, $f(x,t) = t^2 \sin x[\Gamma(4+\gamma)/6 + t^\gamma]$, $L = 2\pi$,

$d_1(x) \equiv 1$, $d_0(x) \equiv 0$, $c(x,t) = t^{3+\gamma}\cos x$. The exact solution is $\theta(x,t) = \sin(x)t^{3+\gamma}$.

For most of finite difference schemes solving the problem with NBCs, the first-order derivatives at the boundaries have to be approximated numerically. Authors in [24] proposed a compact finite difference scheme for this problem by using values of the third-order derivatives of $\theta(x,t)$ at two boundaries, which can achieve the global fourth-order accuracy in space. But for the CCD scheme here, a unified technique is introduced for the derivative boundary conditions. When $T = 1$, for $\gamma = 0.5$ and $\gamma = 0.75$, respectively, the numerical example is computed using the CCD scheme (3.13)–(3.19) with different step sizes in time and a fixed step size $h = \pi/20$. Since the high-order accurate in space the scheme is, the dominated errors are from the approximations of the temporal derivatives. Table 12 gives the computational results and it demonstrates that the convergence order of the CCD scheme (3.13)–(3.19) for the Neumann boundary value problem is $2 - \gamma$ in time.

Table 12: The maximum errors and convergence orders of difference scheme (3.13)–(3.19) in time with a fixed $h = \pi/20$.

τ	$\gamma = 0.5$		$\gamma = 0.75$	
	$E_\infty^{(ND)}(h,\tau)$	$rate_{\infty,\tau}^{(ND)}$	$E_\infty^{(ND)}(h,\tau)$	$rate_{\infty,\tau}^{(ND)}$
1/10	2.441741×10^{-2}	1.41	6.801217×10^{-2}	1.20
1/20	9.194856×10^{-3}	1.44	2.950665×10^{-2}	1.22
1/40	3.390534×10^{-3}	1.46	1.265863×10^{-2}	1.23
1/80	1.233138×10^{-3}	1.47	5.389653×10^{-3}	1.24
1/160	4.444461×10^{-4}	—	2.283556×10^{-3}	—

Next, the numerical accuracy in space is also verified in Table 13 with $\gamma = 0.5$ and $\tau = 1/200,000$. The high-order convergence of the difference scheme (3.13)–(3.19) in space holds based on these data.

Table 13: Maximum errors and convergence orders of difference scheme (3.13)–(3.19) in the spatial direction with $\tau = 1/200,000$, $T = 1$ and $\gamma = 0.5$.

M	$E_\infty^{(ND)}(h,\tau)$	$rate_{\infty,h}^{(ND)}$
4	6.312803×10^{-2}	5.44
8	1.449296×10^{-3}	5.73
16	2.729392×10^{-5}	5.87
32	4.673699×10^{-7}	—

Finally, with $h = \pi/10, \tau = 1/200$ and $\gamma = 0.5$, the long time behavior of numerical solution will be simulated. For $T = 10$, two different schemes are used to compute this example. One is the CCD scheme (3.13)–(3.19), while the other one is the scheme in [24]. Table 13 listed the maximum errors of these two schemes and the error curves are plotted

in Fig. 3. The higher-order accuracy of the difference scheme (3.13)–(3.19) for the problem with NBCs is confirmed. Moreover, with $T = 1$ and $\gamma = 0.5$, taking $\tau^{1.5} \approx h^6$ for the CCD scheme (3.13)–(3.19) and $\tau^{1.5} \approx h^4$ for the scheme in [24], the computational errors in maximum norm and CPU time on the same machine are reported in Table 15, from which, one can see that the effectiveness of the present CCD scheme over the scheme in [24] when the errors are almost in the same magnitudes.

Table 14: The comparison between difference scheme (3.13)–(3.19) and difference scheme in [24] with $h = \pi/10, \tau = 1/200$ for $\gamma = 0.5$.

	difference scheme (3.13)-(3.19)	difference scheme in [24]
T	$E_\infty^{ND}(h,\tau)$	$E_\infty^{ND}(h,\tau)$
1	1.243503×10^{-7}	3.259700×10^{-4}
2	4.779185×10^{-7}	1.302057×10^{-3}
3	1.044951×10^{-6}	3.091389×10^{-3}
4	1.818867×10^{-6}	5.976968×10^{-3}
5	2.798971×10^{-6}	1.032578×10^{-2}
6	4.022370×10^{-6}	1.657404×10^{-2}
7	5.487915×10^{-6}	2.521839×10^{-2}
8	7.851100×10^{-6}	3.711140×10^{-2}
9	1.092445×10^{-5}	6.044885×10^{-2}
10	1.479720×10^{-5}	9.231370×10^{-2}

Table 15: Comparison in the maximum norm errors and CPU time of difference scheme (3.13)–(3.19) and the scheme in [24] with $T = 1$ and $\gamma = 0.5$.

N	difference scheme (3.13)–(3.19)			the scheme in [24]		
	M	$E_\infty^{ND}(h,\tau)$	CPU time (s)	M	$E_\infty^{ND}(h,\tau)$	CPU time (s)
100	20	8.843230×10^{-4}	0.17	35	8.884536×10^{-4}	0.35
200	24	3.191912×10^{-4}	0.35	46	3.196591×10^{-4}	0.56
400	28	1.143730×10^{-4}	0.83	59	1.144005×10^{-4}	1.68
800	33	4.074925×10^{-5}	2.13	77	4.077930×10^{-5}	5.14
1600	40	1.449973×10^{-5}	5.45	100	1.449939×10^{-5}	17.84
3200	47	5.143067×10^{-6}	15.11	130	5.146822×10^{-6}	70.56
6400	56	1.823908×10^{-6}	47.11	168	1.824731×10^{-6}	308.54

5. Concluding remarks

In this paper, several higher-order CCD schemes with the *L1 formula* are proposed to deal with a class of TFADEs. For the constant coefficient problem with the PBCs, a three-

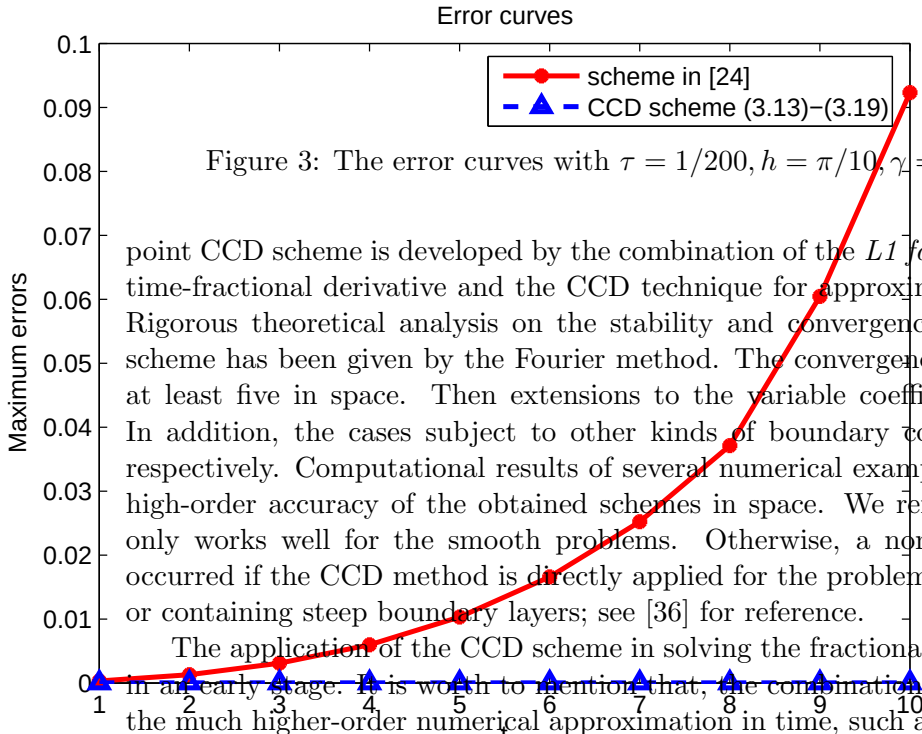

Figure 3: The error curves with $\tau = 1/200, h = \pi/10, \gamma = 0.5$ at different time.

point CCD scheme is developed by the combination of the *L1 formula* for approximating the time-fractional derivative and the CCD technique for approximating the space derivatives. Rigorous theoretical analysis on the stability and convergence of the resulting difference scheme has been given by the Fourier method. The convergence order is $2 - \gamma$ in time and at least five in space. Then extensions to the variable coefficient cases are investigated. In addition, the cases subject to other kinds of boundary conditions are also discussed, respectively. Computational results of several numerical examples confirm the validity and high-order accuracy of the obtained schemes in space. We remark that the CCD method only works well for the smooth problems. Otherwise, a non-physical oscillation can be occurred if the CCD method is directly applied for the problems with non-smooth solutions or containing steep boundary layers; see [36] for reference.

The application of the CCD scheme in solving the fractional differential equations is still in an early stage. It is worth to mention that, the combination of the CCD techniques with the much higher-order numerical approximation in time, such as the *L1-2 formula* proposed in [26], the fractional linear multistep method developed in [27], higher-order Grünwald formula in [28], the weighted and shifted Grünwald formula used in [29], can be considered to improve the numerical accuracy of the obtained numerical schemes in time. However,

rigorous theoretical analysis on the application into FPDEs of the CCD method with these high-order numerical approximation in time is still unavailable. Here, as the starting work of the CCD techniques into solving the FPDEs, the *L1 formula* for approximating the time-fractional derivative is used and strict stability and convergence analysis for the constant coefficient problem with the PBCs are given. Certainly, there is a need on more relevant research on the combination of the CCD techniques with the higher-order discretization for the time-fractional derivatives, and on the further consideration for the fractional wave equations, high-dimensional problems, and other fractional differential equations. In addition, the theoretical analysis on the corresponding schemes for variable coefficient and non-periodic problems will also be our future work.

Acknowledgements

The authors would like to thank Professor Zhi-Zhong Sun for his helpful discussions and to appreciate two anonymous reviewers for their valuable suggestions to greatly improve the manuscript.

Appendix

The proof of (2.6)–(2.7) by Taylor's theorem:

Suppose $u(x) \in C^9[x_{j-1}, x_{j+1}]$. Denote $u'_j = u'(x_j), u''_j = u''(x_j)$, $u'''_j = u'''(x_j), u_j^{(k)} = u^{(k)}(x_j)$. By Taylor's theorem, we have

$$\frac{u_{j+1} - u_{j-1}}{2h} = u'_j + \frac{h^2}{6}u'''_j + \frac{h^4}{5!}u_j^{(5)} + \frac{h^6}{7!}u_j^{(7)} + \mathcal{O}(h^8). \tag{A.1}$$

$$\frac{u''_{j+1} - u''_{j-1}}{2h} = u'''_j + \frac{h^2}{6}u_j^{(5)} + \frac{h^4}{5!}u_j^{(7)} + \mathcal{O}(h^6). \tag{A.2}$$

By (A.1) and (A.2), it follows

$$\begin{aligned}\frac{u_{j+1} - u_{j-1}}{2h} =& u'_j + \frac{h^2}{6}\Big[\frac{u''_{j+1} - u''_{j-1}}{2h} - \frac{h^2}{6}u_j^{(5)} - \frac{h^4}{5!}u_j^{(7)} + \mathcal{O}(h^6)\Big] \\ &+ \frac{h^4}{5!}u_j^{(5)} + \frac{h^6}{7!}u_j^{(7)} + \mathcal{O}(h^8) \\ =& u'_j + \frac{h}{12}(u''_{j+1} - u''_{j-1}) - \frac{7}{360}h^4u_j^{(5)} - \frac{1}{840}h^6u_j^{(7)} + \mathcal{O}(h^8).\end{aligned} \tag{A.3}$$

In addition, it holds

$$\frac{u'_{j+1} + u'_{j-1}}{2} = u'_j + \frac{h^2}{2}u'''_j + \frac{h^4}{4!}u_j^{(5)} + \frac{h^6}{6!}u_j^{(7)} + \mathcal{O}(h^8). \tag{A.4}$$

The application of (A.2) into (A.4) yields

$$\begin{aligned}\frac{u'_{j+1}+u'_{j-1}}{2} =& u'_j + \frac{h^2}{2}\Big[\frac{u''_{j+1}-u''_{j-1}}{2h} - \frac{h^2}{6}u_j^{(5)} - \frac{h^4}{5!}u_j^{(7)} + \mathcal{O}(h^6)\Big] \\ &+ \frac{h^4}{4!}u_j^{(5)} + \frac{h^6}{6!}u_j^{(7)} + \mathcal{O}(h^8) \\ =& u'_j + \frac{h}{4}\Big(u''_{j+1}-u''_{j-1}\Big) - \frac{h^4}{24}u_j^{(5)} - \frac{h^6}{360}u_j^{(7)} + \mathcal{O}(h^8).\end{aligned}$$

The above equality can be rearranged as

$$h^4 u_j^{(5)} = 24u'_j + 6h(u''_{j+1}-u''_{j-1}) - 12(u'_{j+1}+u'_{j-1}) - \frac{h^6}{15}u_j^{(7)} + \mathcal{O}(h^8).$$

Substituting the above expression into (A.3), we find

$$\frac{u_{j+1}-u_{j-1}}{2h} = \frac{1}{30}(7u'_{j+1}+16u'_j+7u'_{j-1}) - \frac{h}{30}(u''_{j+1}-u''_{j-1}) + \frac{h^6}{9450}u_j^{(7)} + \mathcal{O}(h^8). \quad \text{(A.5)}$$

Multiplying 15/8 on both hand sides of (A.5), we have

$$\frac{7}{16}(u'_{j+1}+u'_{j-1}) + u'_j - \frac{h}{16}(u''_{j+1}-u''_{j-1}) = \frac{15}{16h}(u_{j+1}-u_{j-1}) - \frac{1}{5040}u_j^{(7)}h^6 + O(h^8).$$

Thus, (2.6) is obtained.

Similarly, by Taylor's theorem, (2.7) can also be derived easily.

References

[1] S. Das, Functional Fractional Calculus, Springer, Berlin, 2011.

[2] I. Podlubny, Fractional Differential Equations, Academic Press, San Diego, 1999.

[3] A. Kilbas, H. Srivastava, J. Trujillo, Theory and Applications of Fractional Differential Equations, Elesiver Science and Technology, Boston, 2006.

[4] T. Tang, A finite difference scheme for partial integro-differential equations with a weakly singular kernel, Appl. Numer. Math. 11 (1993) 309–319.

[5] M. Meerschaert, C. Tadjeran, Finite difference approximations for two-sided space-fractional partial differential equations, Appl. Numer. Math. 56 (2006) 80–90.

[6] N. Zhang, W. Deng, Y. Wu, Finite difference/element method for a two-dimensional modified fractional diffusion equation, Adv. Appl. Math. Mech, 4 (2012) 496–518.

[7] S. Yuste, L. Acedo, An explicit finite difference method and a new von Neumann-type stability analysis for fractional diffusion equations, SIAM J. Numer. Anal. 42 (2005) 1862–1874.

[8] T. Langlands, B. Henry, The accuracy and stability of an implicit solution method for the fractional diffusion equation, J. Comput. Phys. 205 (2005) 719–736.

[9] F. Liu, P. Zhuang, V. Anh, I. Turner, A fractional-order implicit difference approximation for the space-time fractional diffusion equation, ANZIAM J. 47 (2006) C48–C68.

[10] Z.Z. Sun, X. Wu, A fully discrete difference scheme for a diffusion-wave system, Appl. Numer. Math. 56 (2006) 193–209.

[11] Y. Lin, C. Xu, Finite difference/spectral approximations for the time-fractional diffusion equation, J. Comput. Phys. 225 (2007) 1533–1552.

[12] Y. Lin, X. Li, C. Xu, Finite difference/specrtal approximations for the fractional cable equation, Math. Comp. 80 (2011) 1369–1396.

[13] C. Chen, F. Liu, I. Turner, V. Anh, A Fourier method for the fractional diffusion equation describing sub-diffusion, J. Comput. Phys. 227 (2007) 886–897.

[14] P. Zhuang, Y. Gu, F. Liu et al., Time-dependent fractional advection-diffusion equations by an implicit MLS meshless method, Int. J. Numer. Meth. Engng 88 (2011) 1346–1362.

[15] P. Zhuang, F. Liu, V. Anh, I. Turner, New solution and analytical techniques of the implicit numerical method for the anomalous subdiffusion equation, SIAM J. Numer. Anal. 46 (2008) 1079–1095.

[16] P. Zhuang, F. Liu, V. Anh, I. Turner, Numerical methods for the variable-order fractional advection-diffusion equation with a nonlinear source term, SIAM J. Numer. Anal. 47 (2009) 1760–1781.

[17] C. Chen, F. Liu, I. Turner, V. Anh, Numerical schemes and multivariate extrapolation of a two-dimensional anomalous sub-diffusion equation, Numer. Algor. 54 (2010) 1–12.

[18] M. Cui, Compact finite difference method for the fractional diffusion equation, J. Comput. Phys. 228 (2009) 7792–7804.

[19] R. Du, W. Cao, Z.Z. Sun, A compact difference scheme for the fractional diffusion-wave equation, Appl. Math. Model. 34 (2010) 2998–3007.

[20] G.H. Gao, Z.Z. Sun, A compact finite difference scheme for the fractional sub-diffusion equations, J. Comput. Phys. 230 (2011) 586–595.

[21] X. Hu, L. Zhang, A compact finite difference scheme for the fourth-order fractional diffusion-wave system, Comput. Phys. Comm. 182 (2011) 1645–1650.

[22] X. Hu, L. Zhang, Implicit compact difference schemes for the fractional cable equation, Appl. Math. Model. 36 (2012) 4027–4043.

[23] A. Mohebbi, M. Abbaszadeh, Compact finite difference scheme for the solution of time fractional advection-dispersion equation, Numer. Algor. 63 (2013) 431–452.

[24] J. Ren, Z.Z. Sun, X. Zhao, Compact difference scheme for the fractional sub-diffusion equation with Neumann boundary conditions, J. Comput. Phys. 232 (2013) 456–467.

[25] J. Cao and C. Xu, *A high order schema for the numerical solution of the fractional ordinary differential equations*, J. Comput. Phys. 238 (2013), pp. 154–168.

[26] G.H. Gao, Z.Z. Sun, H. Zhang, A new fractional numerical differentiation formula to approximate the Caputo fractional derivative and its applications, J. Comput. Phys. 259 (2014) 33–50.

[27] F. Zeng, C. Li, F. Liu, I. Turner, The use of finite difference/element approaches for solving the time-fractional subdiffusion equation, SIAM J. Sci. Comput. 35 (2013) A2976–A3000.

[28] C. Li and H. Ding, Higher order finite difference method for the reaction and anomalous-diffusion equation, Appl. Math. Model. (2014) doi:10.1016/j.apm.2013.12.002.

[29] Z. Wang and S. Vong, Compact difference schemes for the modified anomalous fractional sub-diffusion equation and the fractional diffusion-wave equation, J. Comput. Phys. 277 (2014) 1–15.

[30] P. Chu, C. Fan, A three-point combined compact difference scheme, J. Comput. Phys. 140 (1998) 370–399.

[31] P. Chu, C. Fan, A three-point sixth-order nonuniform combined compact difference scheme, J. Comput. Phys. 148 (1999) 663–764.

[32] P. Chu, C. Fan, A three-point sixth-order staggered combined compact difference scheme, Math. Comput. Modelling 32 (2000) 323–340.

[33] T. Nihei, K. Ishii, A fast solver of the shallow water equations on a sphere using a combined compact difference scheme, J. Comput. Phys. 187 (2003) 639–659.

[34] T. Sengupta, V. Lakshmanan, V. Vijay, A new combined stable and dispersion relation preserving compact scheme for non-periodic problems, J. Comput. Phys. 228 (2009) 3048–3071.

[35] T. Sengupta, V. Vijay, S. Bhaumik, Further improvement and analysis of CCD scheme: Dissipation discretization and de-aliasing properties, J. Comput. Phys. 228 (2009) 6150–6168.

[36] J. Zhang, J.J. Zhao, Truncation error and oscillation property of the combined compact difference scheme, Appl. Math. Comput. 161 (2005) 241–251.

[37] G.H. Gao, Z.Z. Sun, Y. Zhang, A finite difference scheme for fractional sub-diffusion equations on an unbounded domain using artificial boundary conditions, J. Comput. Phys. 231 (2012) 2865–2879.

[38] S. Chen, F. Liu, P. Zhuang, V. Anh, Finite difference approximations for the fractional Fokker-Planck equation, Appl. Math. Model. 33 (2009) 256–273.